Pergamon

PII S1359-6454(96)00017-1

Acta mater. Vol. 44, No. 9, pp. 3567–3573, 1996

Published by Elsevier Science Ltd

1359-6454/96 $15.00 + 0.00

EQUILIBRIUM CONTACT ANGLE IN THE MAGNESIUM OXIDE/ALUMINIUM SYSTEM

H. FUJII[1] and H. NAKAE[2]

[1]Department of Materials Science and Metallurgy, University of Cambridge, Pembroke Street, Cambridge CB2 3QZ, England and [2]Department of Materials Science and Engineering, Waseda University, Tokyo 169, Japan

(Received 3 July 1995; in revised form 11 December 1995)

Abstract—The change in the contact angle between two kinds of MgO [sintered sample and single crystal (100) sample] and molten aluminium over time was measured at 1373 K. The atmosphere was a purified He–3vol%H_2 where the formation of the alumina is prevented, and the pressure of the atmosphere was 1.2 atm (1.2×10^5 Pa) to minimise the vaporisation of aluminium. Using a logarithmic time scale, three distinct wetting phases (I, II, III) were easily observed in both systems, as is typical in reactive systems. Phase IV (equilibrium-wetting phase), however, was not observed in the present systems even when the experiment was conducted over a long time. Instead, when investigating the change in interfacial area (interfacial diameter) with the change in contact angle, four detailed stages were observed in phase III (interfacial-reaction-wetting phase). These stages in phase III were caused by a decrease in the volume of the molten aluminium due to the interfacial reaction and the vaporisation of the drop. The progress through the stages represented a transition in contact angle from an advancing contact angle to a receding contact angle. In systems where the decrease in volume is too great, the equilibrium contact angle cannot be obtained directly. Here, a method is proposed for the estimation of the equilibrium contact angle in such a system. *Copyright © 1996 Acta Metallurgica Inc.*

1. INTRODUCTION

The wetting of ceramics by molten metal is one of the most important phenomena in metallurgical process industries where molten metal is used, and values for contact angles are required in many fields such as in the fabrication of metal matrix composites, melting and casting of metals and bonding of ceramics to metals. For this reason, the contact angle between various ceramic samples and molten metal have been measured by many researchers [1–4].

Although the principle of the measurement of contact angle is simple, it is not very easy to measure the contact angle precisely in ceramic–aluminium systems. One of the reasons is the oxidation of aluminium [5, 6]. When an oxide film exists on the surface of the aluminium, it is likely that the oxide film will prevent the interface from moving, resulting in incorrect values for the contact angle being obtained.

Another reason is that the reactivity of aluminium is so high that the interfacial reaction usually changes the contact angle with time. In a reactive system, the wetting progresses through four phases (I: original-wetting phase, II: quasi-equilibrium phase, III: interfacial-reaction-wetting phase, IV: equilibrium phase) [7, 8]. However, these wetting phases are not easily found on a linear time scale: it is only when a logarithmic time scale is used, that they become apparent [9, 10]. Therefore, the wetting phase in which the contact angles are measured has varied according to the researchers, and most of the contact angles have been measured in phases III or IV, not phases I or II.

We previously investigated the wetting of MgO by molten aluminium [10, 11] and the original contact angle (phase II) was measured. At this time the equilibrium contact angle was not obtained because the experimental time was too short. In the present study, then, the change in contact angle was measured for a longer time. However, it has become clear that phase IV can never be observed in this system. Instead, four detailed stages were observed in phase III. The physical meaning of these phenomena is discussed below. In addition, a method is proposed for the estimation of the equilibrium contact angle in such a system.

As with the previous measurements [10, 12], an improved sessile drop method preventing the formation of alumina was used in order to obtain more accurate values for the contact angle.

2. EXPERIMENTAL APPARATUS AND PROCEDURE

The sessile drop method has been widely used to measure the wetting of various materials. In ceramic–metal systems the metal in a solid state is usually placed on the ceramic surface before heating. Then, the sample is heated to melt the metal on the ceramic surface. While the sample is being heated, the

ceramic surface reacts with the metal, preventing the original contact angle (the contact angle of the original system) from being measured. In addition, when this conventional sessile drop method is applied to the measurement of wetting by aluminium, the oxidation of aluminium cannot be prevented.

When the initial oxide film is removed and the partial pressure of Al_2O is lower than 2.46×10^{-2} Pa at 1373 K [12], the following reaction

$$Al(l) + Al_2O_3(s) \rightarrow 3Al_2O(g) \quad (1)$$

occurs, and thus the formation of alumina can be prevented [13]. In the conventional sessile drop method, however, as the initial Al_2O_3 film remains on the aluminium surface and is impermeable, the gas phase Al_2O is unable to escape and thus the reaction cannot occur: hence the importance of removing the initial oxide film. To achieve this, an improved sessile drop method was devised, incorporating an aluminium dropping device. This has been described in detail elsewhere [10, 12].

The system consists of a sealed chamber, a purification system for the atmospheric gas (He–3%H_2) in the chamber, a set of vacuum pumps to evacuate the chamber, two light sources and two cameras: a 35 mm camera and a video recording camera both with bellows and macro lenses. The sealed chamber has four windows and contains a molten aluminium dropping device and a molybdenum cylindrical heater with three concentric reflectors located around the dropping device.

The gas purification system consists of a molecular sieve, an oxygen trap, two liquid nitrogen cold traps and an titanium furnace to remove H_2O and O_2 from the atmospheric gas. One liquid nitrogen cold trap was placed before the titanium furnace and the other after it in order to trap the furnace vapour as well as any extra H_2O.

The experiments were conducted using 99.99 mass% aluminium pellets as the metal. The aluminium pellets weighted approximately 70 mg each and were pretreated by immersion in hydrofluoric acid and then in acetone. Sintered MgO and single crystal MgO (100) were used as substrates. The chemical composition of the MgO samples [10, 11] is shown in Table 1. The sintered ceramic plates were polished to a mirror finish using various grades of SiC paper and two grades of diamond paste (particle diameter 6 and 0.25 μm). The single crystal was cleaved along the surface (100). The plates were cleaned before the experiments in acetone using an ultrasonic cleaner.

Table 1. Chemical composition of the sintered MgO

Sample	MgO	SiO_2	CaO	Fe_2O_3	Al_2O_3
Sintered MgO	96.85	1.71	0.83	0.05	0.03
Single crystal (100)	99.9	tr.	tr.	tr.	tr.

A ceramic plate was set in a horizontal position under the dropping device, and the chamber then evacuated to 1.3×10^{-4} Pa (approximately 10^{-6} Torr) and heated to 1423 K. This temperature was maintained for about 3600 s to remove hydroxyl group [14] before the purified He–3%H_2 atmospheric gas was introduced and the pressure raised to 120 kPa (1.2 atm). The chamber was then cooled to the requisite experimental temperature and an aluminium pellet placed outside the furnace was dropped into the bottom of the dropping device. On reaching the requisite experimental temperature, the aluminium is, as a liquid, slowly forced through the hole in the base of the tube by a gradual decrease in the atmospheric pressure of the chamber. At this time, the initial oxide film is removed mechanically by the action of passing through the hole, and initial wetting begins.

The contact angles θ were measured using projections of the 35 mm monochrome negatives (magnification 50×). When θ was greater than 100°, the value was calculated using Bashforth and Adams's tables [15]. When θ was less than 100°, the contact angles were measured directly on the projections because the contact angle values obtained using Bashforth and Adams' table contain a margin of error.

3. EXPERIMENTAL RESULTS

Figure 1(a) shows the change in the contact angle and the change in the interfacial diameter, $2x$, for the sintered MgO/Al, on the logarithmic time scale. Figure 1(b) shows the same results on a linear time scale. The temperature is 1373 K. It can be seen on a logarithmic time scale that there are three initial wetting phases (I: original-wetting phase, II: quasi-equilibrium phase, III: interfacial-reaction-wetting phase) [7, 8] as in typical reactive systems such as Hg/Cu [9], BN/Al(–Si) [12, 13], SiC/Al(–Si) [16], Si_3N_4/Al [17] and C/Al(–Si) [18]. However, in this system, unlike in the above mentioned ones, Phase IV (equilibrium phase) cannot be observed. A steady contact angle is not observed until the contact angle decreases to 0°, that is, until the liquid disappears [19].

The original wetting is the physical wetting for the original system (before interfacial reactions), which can also be observed in a non-reactive system. This wetting is very fast and finishes in much less than 1 s for the aluminium at 1373 K, according to the video recording observation [20]. The interfacial-reaction wetting is the wetting caused by the interfacial reactions. The rate of the interfacial-reaction wetting is much less than that of the original wetting (less than 1/1000 in this system). This is the reason why the two wettings can be separated using a logarithmic time scale.

Figures 2(a) and (b) show the changes in contact angle and interfacial diameter, $2x$, in the single

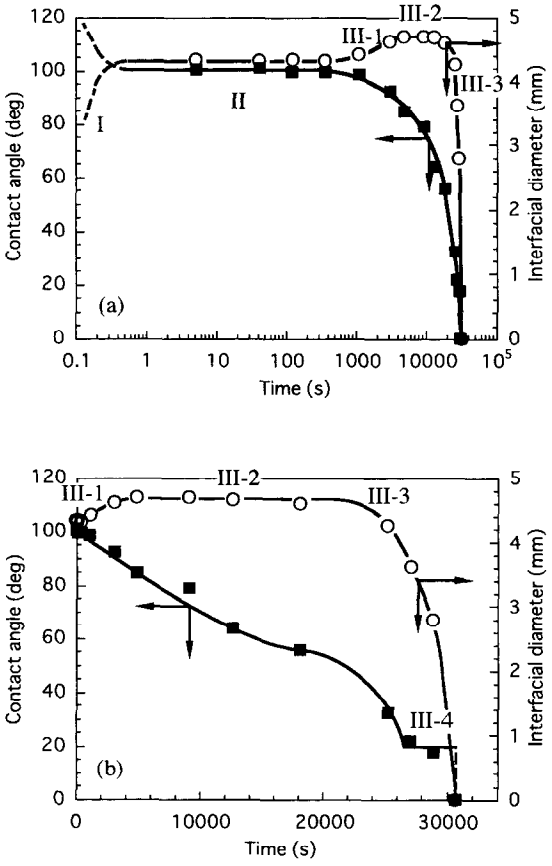

Fig. 1. Changes in contact angle and interfacial diameter for the sintered MgO–Al at 1373K. (a) Logarithmic time scale; (b) linear time scale.

crystal MgO (100) and Al system, on a logarithmic time scale and on a linear time scale, respectively. The temperature is again 1373 K. Figure 2(a) also shows three wetting phases, as in the sintered MgO–Al system. Phase IV, however, cannot be observed in this system, either.

4. DISCUSSION

4.1. Mechanism of interfacial-reaction wetting

As mentioned in the previous chapter, the difference in the rate of the original wetting and the interfacial-reaction wetting, enables us to separate the two wettings using a logarithmic time scale. This indicates that, during the progress of the interfacial-reaction wetting, the mechanical equilibrium is achieved over any short time period and the change in contact angle represents the change in the condition of the interface. It has to be pointed out that the interfacial reaction cannot improve the mechanical wetting and only affects the condition of the interface, resulting in a change in contact angle.

It is confirmed experimentally that the progress of the interfacial-reaction wetting is determined by the change in the condition of the interface (strictly speaking the condition of the three phase line) [12, 21]. For example, the oxygen included AlN–Al system produces Al_2O_3 at the interface and the contact angle changes with time. As the ratio of Al_2O_3 increases, the contact angle decreases. This is because the equilibrium contact angle of Al_2O_3–Al (89° at 1373 K) is less than that of AlN–Al (128°at 1373 K). The interface during the interfacial-reaction wetting can be regarded as a kind of composite material [12, 21], and the progress of the wetting can be explained using Cassie's equation [22]. In an impure system, of course, the segregation of impurities can also change the condition of the interface, resulting in the production of a driving force for the wetting.

In the present single crystal MgO–Al system α-Al_2O_3 is produced at the interface, as reported in the previous paper [11]. The interfacial reaction is considered to be as follows

$$2Al(l) + 3MgO(s) \rightarrow 3Mg(l) + Al_2O_3(s). \quad (2)$$

Thus, the production of Al_2O_3 at the interface and the increase in magnesium in the aluminium drop change the condition of the interface and lead to a change in contact angle.

In the sintered MgO–Al system [10, 11], on the

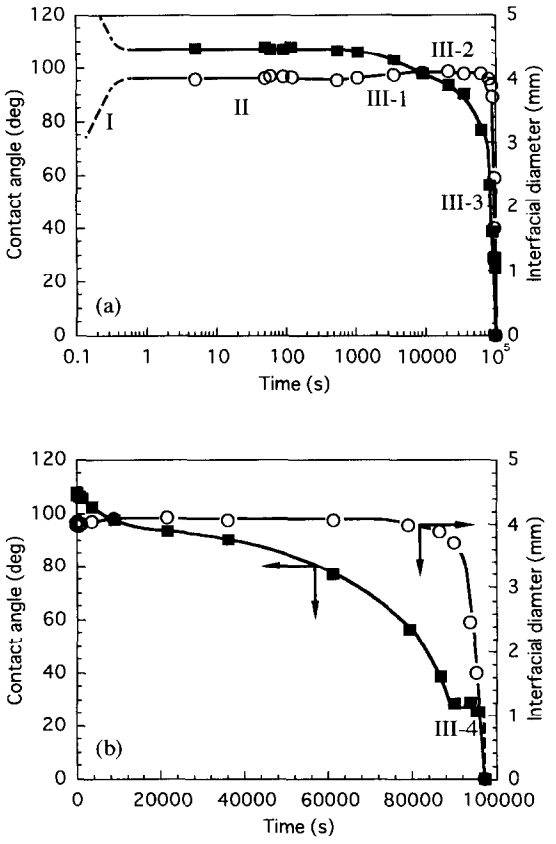

Fig. 2. Changes in contact angle and interfacial diameter for the single crystal MgO (100) at 1373K. (a) Logarithmic time scale; (b) linear time scale.

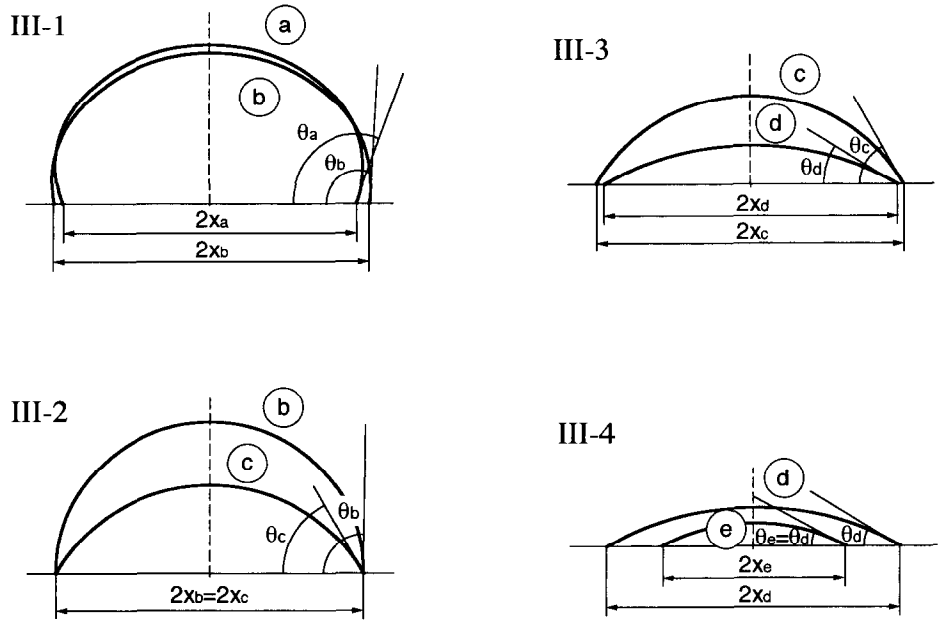

Fig. 3. Schematic model of the change in drop during phase III.

other hand, the interfacial reaction is expressed as follows

$$2Al(l) + 4MgO(s) \rightarrow 3Mg(l) + MgO \cdot Al_2O_3(s). \quad (3)$$

In this case, the production of $MgO \cdot Al_2O_3$ at the interface, the increase in magnesium in the aluminium drop and the segregation of the impurity of ceramics, in particular calcium at the interface, change the condition of the interface and cause the contact angle to change.

However, at the certain point in phase III, 7200 s, in the single crystal MgO–Al, Al_2O_3 already extends beyond the three phase line and the depth of the reaction zone is about 80 μm [11]. In addition, on analysing the composition of the drop of the quenched sample, the quantity of magnesium in the drop was found to be very small (380 ppm) [11]. This is because the vaporisation pressure of magnesium is very high, as mentioned later.

In the sintered MgO–Al sample, also, the interfacial reaction extended beyond the three phase line and the depth of the reaction zone was about 860 μm [11] after 7200 s. The content of magnesium in the drop after 7200 s was 330 ppm, which was very close to the quantity in the single crystal MgO–Al system in spite of the difference in the rate of the interfacial reaction. Thus, the quantity of magnesium in the aluminium seems to have already reached equilibrium in both systems at that time. The segregation layer of calcium of the sintered MgO–Al system is approximately 25 μm, which is probably big enough to conclude that the concentration of calcium at the top layer of the interface does not change very much later.

Therefore, a few atomic layers at the interface, which are likely to determine the wetting do not change much after 7200 s in either system. Accordingly, the total free energy does not change with the movement of the three phase line. Thus, the decrease in the contact angle after phase III-2 seems not to depend on the interfacial reaction. As discussed in the next section, it is dependent on the degree of decrease in the drop volume.

4.2. *Four stages in phase III*

Why was the equilibrium contact angle not observed? When the change in the interfacial diameter, $2x$, is investigated, it is found that there are four distinct stages in phase III (1, 2, 3, 4) as shown in Figs 1 and 2. The contact angle continues decreasing throughout all the stages of phase III. However, the interfacial area increases in phase III-1, becomes constant in phase III–2 and then decreases in phase III-3 and 4. Figure 3 shows the schematic model of the change in drop during phase III.

Phase III–1 is an advancing contact angle phase because the interface is advancing. Phase III-3 is, on the other hand, a receding contact angle phase because the interfacial diameter is decreasing. Therefore, it seems that, in phase III–2, the contact angle changes from an advancing contact angle to a receding contact angle by way of the equilibrium contact angle.

When a logarithmic time scale is used, the contact angle continues decreasing to 0° without any

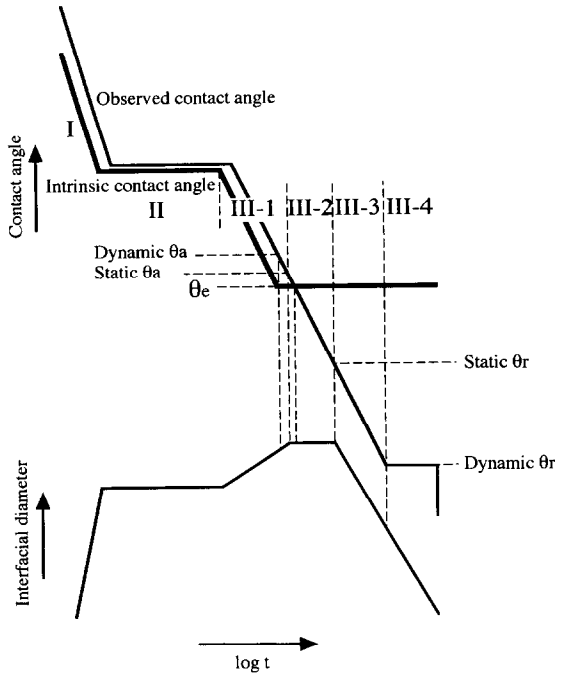

Fig. 4. A model of the changes in apparent contact angle and intrinsic contact angle. (θ_a: advancing contact angle; θ_r: receding contact angle; θ_e: equilibrium contact angle.)

suspension because the schematic range is small for results obtained such a long time after dropping. However, when a linear time scale is used, a phase can be seen where the contact angle is constant though the interfacial diameter is decreasing (phase III-4). The contact angle in phase III-4 is a "true" receding contact angle of the system because the interface is actually receding with a constant contact angle.

The change in the state of each stage in phase III is summarised in Table 2.

The decrease in the contact angle, at least from the middle of phase III-2, is caused by hysteresis, not an intrinsic change. The hysteresis, the difference between the advancing contact angle and the receding contact angle, is caused by the surface roughness. When the solid surface is perfectly flat, there is no hysteresis. In real systems, however, surface roughness, and thus hysteresis, exists, though in some cases they may be negligible. When the interface is advancing the observed contact angle becomes larger. When the interface is receding, on the other hand, the observed contact angle becomes smaller [23].

When the surface roughness is greater, the hysteresis also becomes greater. In this study, in order

Table 3. Surface roughness (R_a) after the interfacial reaction (μm)

	Solid–vapour interface[a]	Solid–liquid interface[b]
Sintered MgO–Al	4.0	11.5
Single crystal MgO–Al	2.0	5.5

[a]The values were measured 7200s after dropping.
[b]The values were measured after each wetting experiment.

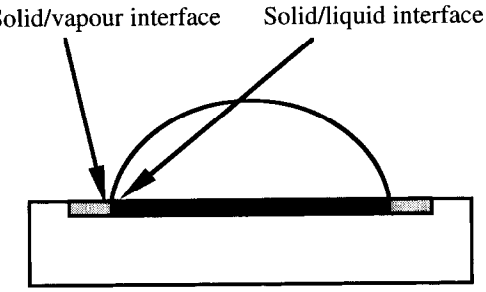

to minimise the hysteresis, the surface of the ceramics was carefully polished, as mentioned before. However, during the experiment, the ceramic surface roughens due to the chemical reactions, as shown in Table 3. In particular, the roughness of the solid–liquid interface becomes greater because of greater reactions. Accordingly, the difference from the intrinsic contact angle should be greater when the interface is receding. As a reference, the surface roughness of the solid–liquid interfaces was measured after each wetting experiment and the surface roughness of the solid–vapour interfaces was measured for the sample when the wetting experiment had been stopped 7200 s after dropping.

V. de Jonghe *et al.* reported that when the surface roughness (R_a) is 0.52 μm in Al_2O_3–Al, the difference between the advancing contact angle and the receding contact angle is 61° at 1073 K [24]. In this study, because the surface roughness is greater than 0.52 μm due to the interfacial reactions, greater hysteresis can occur and the differences in the contact angle, 68° (88 − 20°) in the sintered MgO–Al and 69° (97 − 28°) in the single crystal MgO–Al, are reasonable.

Figure 4 shows a model of the changes in the apparent contact angle and the intrinsic contact angle. This model is based on the fact that when the three phase line (solid–liquid–vapour interface) is advancing, the apparent contact angle is greater than the intrinsic contact angle, and that when the three phase line is receding, the apparent contact angle is smaller than the intrinsic contact angle. According to

Table 2. Change in the state of each stage in phase III

	Contact angle	Interfacial area	State of contact angle
III–1	Decreasing	Increasing	θ_a
–2	Decreasing	Constant	Shifting from θ_a to θ_r
–3	Decreasing	Decreasing	θ_r
–4	Constant	Decreasing	"true" θ_r

θ_a: advancing contact angle; θ_r: receding contact angle.

Table 4. Summary of the change in contact angle

	Static θ_a	Static θ_r	Dynamic θ_r	Calculated θ_e
Sintered MgO	88°	55°	20°	79°
Single crystal MgO	97°	56°	28°	86°

Rivollet [25], even when the three phase line stops after the advance, the contact angle is still greater than the intrinsic contact angle because the three phase line cannot go over the "mountain" of the surface. Similarly, when the three phase line stops after the receding, the contact angle is smaller than the intrinsic contact angle. However, the receding contact angle at this time is larger than the receding contact angle while the three phase line is actually receding, even when the speed is only 0.01 mm/min [25].

Accordingly, we have named the contact angle when the three phase line starts to recede or finishes receding a static receding contact angle, and the contact angle when the three phase line is receding a dynamic receding contact angle. The static receding contact angle corresponds to the value at the beginning of phase III-3, judging from the change in $2x$, and the dynamic contact angle corresponds to the value observed in phase III-4. On the other hand, the value of the starting point of phase III-2 corresponds to the static advancing contact angle, assuming that the changes in the condition of the interface have already finished at this time. In addition, although a dynamic advancing contact angle is not observed, if it exists, it should be before the static advancing contact angle because the contact angle must be larger when the three phase line is moving.

4.3. Estimation of equilibrium contact angle

In order to obtain the equilibrium contact angle, the hysteresis has to be minimised. In order to iminimise the hysteresis, the surface of the substrate has to be polished carefully to minimise the surface roughness. However, in a reactive system, the interfacial reactions usually roughen the surface, which is inevitable.

Another way of obtaining the equilibrium contact angle is to prevent the contact angle from shifting to the receding contact angle. To achieve this, the vaporisation of the liquid has to be minimised. Using an atmospheric gas rather than a vacuum diminishes the decrease in drop volume. Because the contact angle is usually not measured near the boiling point of the liquid, the vaporisation pressure is not so high and this method is effective. In fact, in this system, the vaporisation pressure of aluminium is not high (2.4×10^{-1} Pa) [26] at the experimental temperature of 1373 K.

However, in this system, the vaporisation pressure of magnesium is close to 1 atm (1.0×10^5 Pa) because the boiling point of Mg is 1380 K, which is only 7 K higher than the experimental temperature, 1373 K. Therefore, the produced Mg easily escapes from the system though the aluminium does not. Actually, powdered Mg was observed on the wall of the chamber after the experiment, as reported in the previous paper [10, 11]. Accordingly, it is concluded that the decrease in the drop volume due to the vaporisation of magnesium is too large to produce an equilibrium contact angle. In a system where the quantity of the liquid decreases substantially due to the interfacial reaction, such as with MgO–Al, it is believed that the equilibrium contact angle cannot be obtained directly. Therefore, it is necessary to estimate the equilibrium contact angle indirectly.

The summary of data is shown in Table 4. The equilibrium contact angle must exist between the static advancing contact angle and the static receding contact angle. The magnitude of the difference between the equilibrium contact angle and the static advancing contact angle and that between the equilibrium contact angle and static receding contact angle depends on the magnitude of the surface roughness. Therefore, because the roughness of a solid–liquid interface is larger than that of a solid–vapour interface, as shown in Table 3, the difference between the equilibrium contact angle and the static receding contact should also be larger.

Here, assuming the hysteresis, (the difference in the cosine of the contact angles) is proportional to the magnitude of the roughness, the equilibrium contact

Table 5. Change in the observed contact angle

Phase	From	To	by way of
I	Dynamic θ_a of S_o/L_o	Static θ_a of S_o/L_o	
II	Static θ_a of S_o/L_o	Static θ_a of S_o/l_o	
III-1	Static θ_a of S_o/L_o	Static θ_a of S_e/L_e	
III-2	Static θ_a of S_e/L_e	Static θ_r of S_e/L_e	Equilibrium contact angle
III-3	Static θ_r of S_e/L_e	Dynamic θ_r of S_e/L_e	
III-4	Dynamic θ_r of S_e/L_e	Dynamic θ_r of S_e/L_e	

θ_a: advancing contact angle; θ_r: receding contact angle; S_o/L_o: the solid–liquid interface of the original system; S_e/L_e: the soild–liquid of the equilibrium system.

angle was estimated. Although the surface roughness was not measured at the most suitable time, the values in Table 3 were used, assuming the difference is not very great. The estimated equilibrium contact angle values were 79° for the sintered MgO–Al system and 86° for the single crystal MgO–Al system. The latter value is close to the equilibrium contact angle of 89° for Al_2O_3–Al [21], indicating the estimation is not so bad.

Because the relationship between the surface roughness of the substrate and the hysteresis of the contact angle is still not completely clear, a simple assumption was made in this study that hysteresis is proportional to the roughness. Of course, an attempt can be made to estimate the value more precisely by measuring the surface roughness carefully at the correct time and by using a better relationship between the surface roughness and the hysteresis, such as the relationship proposed by de Jonghe *et al.* [24].

In summary, in order to obtain a satisfactory value for the equilibrium contact angle, it is necessary to polish the substrate carefully and not to measure the contact angle in a vacuum. However, even when these conditions are obtained, in a system where the quantity of liquid decreases substantially due to the interfacial reaction, such as with MgO–Al, it is not likely that the equilibrium contact angle can be obtained directly. In such cases, it is necessary to use an indirect estimation method such as that proposed in this section.

5. SUMMARY

The change in the contact angle between two types of MgO [96.85mass % sintered and single crystal (100)] and molten aluminium over time was measured at 1373 K. The following results were found.

1. The change in contact angle with time in both MgO–Al systems has three phases (I: original–wetting phase, II: quasi-equilibrium phase, III: interfacial-reaction-wetting phase), similar to typical reactive systems.

2. Phase IV (equilibrium-wetting phase), however, is not observed in either system. Thus, although the contact angle of the original system (before the interfacial reactions) can be measured in phase II, the intrinsic contact angle after the interfacial reactions (equilibrium contact angle) cannot be measured.

3. Instead, on investigating the change in the interfacial area, four different stages are observed in phase III.

III-1: contact angle decreases with an increase in interfacial area;

III-2: contact angle decreases with a constant interfacial area;

III-3: contact angle decreases with a decrease in the interfacial area;

IV-4: contact angle remains constant with a decrease in the interfacial area.

4. The four stages in phase III are caused by the fact that the contact angle shifts from an advancing contact angle to a receding contact angle. The change in the observed contact angle in each phase can be summarised as shown in Table 5.

5. Thus, in a system where the quantity of the liquid decreases substantially due to the interfacial reactions, such as in MgO–Al, the equilibrium contact angle cannot be observed.

6. The equilibrium contact angle was therefore estimated using the static advancing contact angle and the static receding contact angle taking into account the surface roughness. The values obtained for 96.85 mass% sintered MgO–Al and single crystal (100)–Al were 79 and 86°, respectively.

REFERENCES

1. Y. Naidich, *Prog. Surf. Membr. Sci.* **14,** 353 (1981).
2. V. Laurent, D. Chatain, C. Chatillon and N. Eustathopoulos, *Acta metall.* **36,** 1797 (1988).
3. J. E. McDonald and J. G. Eberhart, *Trans. Metall. Soc. AIME* **233,** 512 (1965).
4. S. K. Rhee, *J. Amer. Ceram. Soc.* **53,** 639 (1970).
5. H. John and H. Hausner, *J. Mater. Sci. Lett.* **5,** 549 (1986).
6. D. Wang and S. Wu, *Acta metall. mater.* **42,** 4029 (1994).
7. H. Nakae, H. Fujii and K. Sato, *Mater. Trans. JIM* **33,** 400 (1992).
8. O. M. Akselsen, *J. Mater. Sci.* **27,** 1989 (1992).
9. H. Nakae, H. Yamaura, Y. Shinohara, K. Yamamoto and Y. Oosawa, *Mater. Trans. JIM* **30,** 423 (1989).
10. N. Yoshimi, H. Nakae and H. Fujii, *Mater. Trans. JIM* **31,** 141 (1990).
11. H. Fujii and H. Nakae, *ISIJ Int.* **30,** 1114 (1990).
12. H. Fujii, H. Nakae and K. Okada, *Acta metall. mater.* **41,** 2963 (1993).
13. S. J. Park, H. Fujii and H. Nakae, *J. Jpn Inst. Metals* **58,** 208 (1994).
14. J. J. Brennan and J. A. Pask, *J. Amer. Ceram. Soc.* **51,** 569 (1968).
15. F. Bashforth and J. C. Adams, *An Attempt to Test the Theories of Capillary Action*, p. 82. Cambridge University Press, London (1883).
16. K. Sato and H. Nakae, *J. Japan Inst. Light Metals* **41,** 841 (1991).
17. M. Midorikawa, M. Saito, H. Fujii and H. Nakae, *Abstracts of the 1990 Autumn Meeting of J. Jpn Inst. Light Metals*, 135 (1990).
18. H. Nakae, K. Yamamoto and K. Sato, *Mater. Trans. JIM* **32,** 531 (1991).
19. A. J. McEvoy, R. H. Williams and I. G. Higginbotham, *J. Mater. Sci.* **11,** 297 (1976).
20. H. Fujii, Ph.D Thesis Waseda University, 65 (in Japanese) 63 (in English) (1993).
21. H. Fujii, H. Nakae and K. Okada, *Metall. Trans.* **24A,** 1391 (1993).
22. A. B. D. Cassie, *Discussions Faraday Soc.* **3,** 11 (1948).
23. R. E. Johnson, Jr and R. H. Dettre, *Contact Angle, Wettability and Adhesion* (edited by F. M. Fowkes), p. 112. Amer. Chem. Soc. (1964).
24. V. de Jonghe, D. Chatain, I. Rivollet and N. Eustathopoulos, *J. Chim. Phys.* **87,** 1623 (1990).
25. I. Rivollet, D. Chatain and N. Eustathopoulos, *J. Mater. Sci.* **25,** 3179 (1990).
26. O. Kubaschewski and C. B. Alcock, *Metallurgical Thermochemistry*, 5th ed., 358 (1979).